Available online at www.sciencedirect.com
ScienceDirect
Trans. Nonferrous Met. Soc. China 20(2010) s435−s438
Transactions of Nonferrous Metals Society of China
www.tnmsc.cn

Microstructure and mechanical properties of die-cast AZ91D magnesium alloy by Pr additions

CUI Xiao-peng(崔晓鹏)[1, 2], LIU Hai-feng(刘海峰)[3], MENG Jian(孟 健)[2], ZHANG De-ping(张德平)[2]

1. Department of Materials Science and Engineering, Key Laboratory of Advanced Structrural Materials of Ministry of Education, Changchun University of Technology, Changchun 130012, China;
2. State Key Laboratory of Rare Earth Resources Utilization, Changchun Institute of Applied Chemistry, Chinese Academy of Sciences, Changchun 130022, China;
3. R&D Centre of Foundry Corporation, FAW Group Corporation, Changchun 130062, China;

Received 23 September 2009; accepted 30 January 2010

Abstract: Mg-9Al-*x*Pr (*x*=0.4, 0.8 and 1.2, mass fraction, %) magnesium alloys were prepared by high-pressure die-casting technique. The effects of Pr on the microstructures of die-cast Mg-9Al based alloy were investigated by XRD and SEM. Needle-like $Al_{11}Pr_3$ phase and polygon Al_6Mn_6Pr phase are found in the microstructure. With 0.4% Pr addition, fine needle-like $Al_{11}Pr_3$ phase and a small amount of polygon Al_6Mn_6Pr phase near the grain boundary are found in the microstructure. Increasing Pr addition to 0.8%, lots of coarse needle-like $Al_{11}Pr_3$ phase within grain and polygon Al_6Mn_6Pr phase on grain boundary are observed. Further increasing Pr addition, the size of needle-like $Al_{11}Pr_3$ phase decreases, while the size of polygon Al_6Mn_6Pr relatively increases. The mass fraction of Pr at around 0.8% is considered to be suitable to obtain the optimal mechanical properties. The optimal mechanical properties are mainly resulted from grain boundary strengthening obtained by precipitates and solid solution.
Key words: praseodymium; magnesium alloy; microstructure; mechanical properties

1 Introduction

Due to the lower density, more and more magnesium alloy parts produced by high pressure die casting are applied to automobile industry. Some commercial Mg-Al alloys, such as AZ91D, AM60B and AM50A, have already been introduced into certain automobile parts of instrument panel, seat frame, steering wheel and so on[1]. Compared with steel and aluminum alloy, magnesium alloy is restricted in further application in the automobile field for its poor strength. Improving magnesium alloy strength by adding the rare earth elements is the most effective means. RE can be found in most new high-strength magnesium alloys which are currently developed[2−11]. Moreover, mixed rare-earth master alloy (Ce-La-Pr-Mg)[12−13] is often used for the development of Mg-RE alloy in most study. Pr has been usually used for the development of high-strength magnesium alloy. But Pr addition in Mg-RE alloy is always accompanied with other rare earth elements (the main elements are Ce and La) because there are interactions among different rare earth elements. They can lead to misunderstanding on the effect of Pr addition on the microstructure. There are few reports about the effect of single Pr addition on the magnesium alloy microstructure and mechanical properties. It is important to investigate the effect of single Pr addition on the microstructure and strengthening mechanism for new magnesium alloy design. This work has focused on the effect of single Pr addition on the microstructure and mechanical properties of Mg-9Al base alloy and tries to find its mechanism.

2 Experimental

Considering good castability, Mg-9Al base alloy was selected as basic alloy to develop the new alloy. Commercial AZ91D, pure Mg, Al, Mg-20%Pr master alloy and Al-10%Mn master alloy were used to fabricate

Foundation item: Project(2006AA03Z520) supported by National High-tech Research and Development Program of China; Project(20080508) supported by the Science and Technology Program of Jilin Province of China; Project(2007094) supported by the Science and Technology Program of Education Department of Jilin Province of China; Project(2007101) supported by the Science & Technology Development Program; Project supported by the Basic Research Program of Changchun University of Technology, China
Corresponding author: CUI Xiao-peng; Tel: +86-13180826670; E-mail: cuixiaopeng2004@126.com

Mg-9Al-*x*Pr alloys. The chemical compositions of the alloys were determined by inductively coupled plasma atomic emission spectroscopy (ICP-AES) and the results are listed in Table 1.

Table 1 Chemical composition of studied alloy

Alloy	Mass fraction/%				
	Al	Mn	Pr	Zn	Mg
Mg-9Al-0.4Pr	9.25	0.48	0.39	0.62	Bal.
Mg-9Al-0.8Pr	9.01	0.39	0.84	0.58	Bal.
Mg-9Al-1.2Pr	8.94	0.42	1.15	0.55	Bal.

The magnesium alloy melt was prepared at a steel crucible with melt capacity of 20 kg. A 630 t cold-chamber die casting machine was used to cast the metal into a four-cavity die producing two tensile bars of 6 mm in diameter and 100 mm in gage length, and two tensile creep bars of 10 mm in diameter and 100 mm in gage length. For the entire casting trial, the melt temperature was not exceed 780 ˚C in alloying, and was controlled at 650−660 ˚C in die casting. For each alloy composition, at least 15 shots were made. The mechanical properties tests were carried out at room temperature and the value was the average of at least 4 measurements. Metallographic samples were cut from the middle segments of the tensile or creep bars. To reveal microstructure, the specimen surfaces were etched with 4% nitric acid solution. The microstructure of sample was observed by using scan electron microscopy (JSM-5600lv) equipped with an X-radiation detector EDS. EDS analysis was performed with an accelerating voltage of 15 keV. The phase identification of these alloys was conducted by X-ray diffraction (D-MAXLL A) using Cu K_α radiation.

3 Results and discussion

3.1 Analysis of microstructures

The XRD patterns of Mg-9Al-*x*Pr alloys indicate that the alloys are mainly composed of α-Mg phase and $Mg_{17}Al_{12}$ phase (Fig.1). The intensities of α-Mg peaks are not proportional to the data from PDF cards, indicating the random distribution of grain orientations. The other diffraction lines are identified as Al_6Mn_6Pr and $Al_{11}Pr_3$. The increase of Pr content from 0.8% to 1.2% leads to a XRD pattern change of Mg-9Al alloys (Figs.1(a)−(c)). While Pr addition is 0.4%, the main intermetallic phase is $Al_{11}Pr_3$, and its reflection is low (Fig.1(a)). With the increasing of Pr addition, the reflection intensity of $Al_{11}Pr_3$ phase increases, and Al_6Mn_6Pr phase can be identified in XRD pattern (Figs.1(b)−(c)).

The microstructures of Mg-9Al-*x*Pr alloys under SEM microscope are shown in Fig.2, and EDS results are shown in Table 2. The α-Mg matrix, divorced eutectic, few kinds of precipitations can be observed in the microstructure. The grain size of the three kinds of

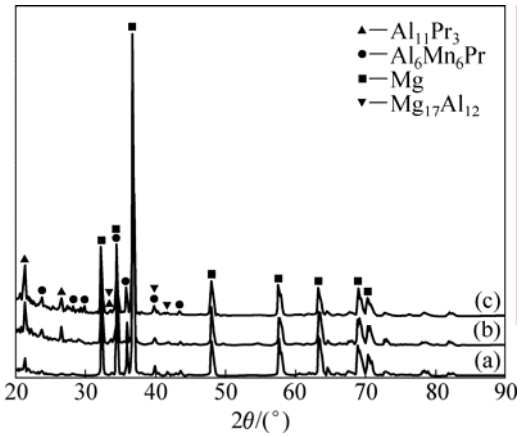

Fig.1 X-ray diffraction patterns of Mg-9Al-*x*Pr alloys: (a) Mg-9Al-0.4Pr; (b) Mg-9Al-0.8Pr; (c) Mg-9Al-1.2Pr

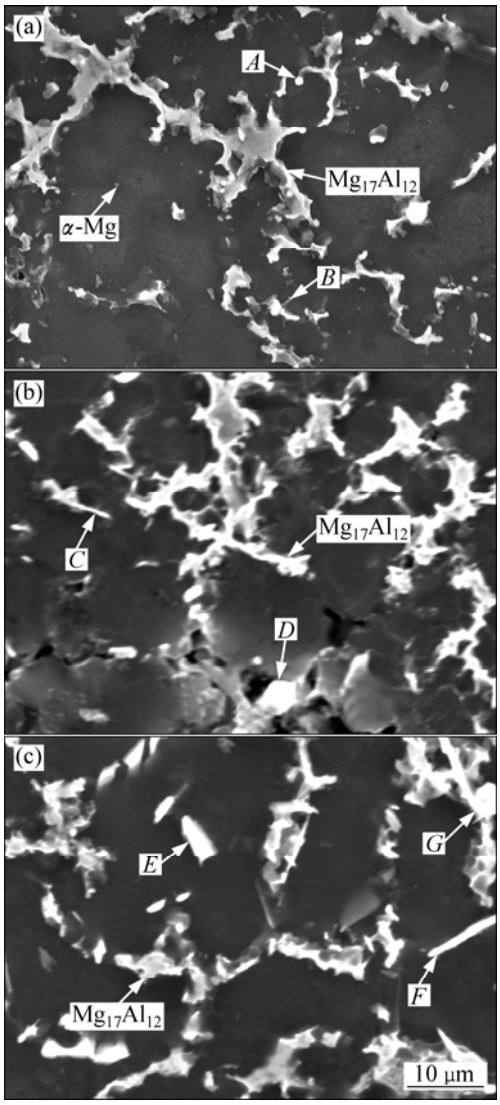

Fig.2 SEM images of die-casting alloys: (a) AZ91+0.4Pr; (b) AZ91+0.8Pr; (c) AZ91+1.2Pr

Table 2 EDS analysis results of points in Fig.2

Point	Mole fraction/%			
	Mg	Al	Pr	Mn
A	5.65	45.38	8.43	40.54
B	15.78	67.85	16.37	−
C	32.63	49.27	18.1	−
D	12.35	36.45	6.38	44.82
E	25.43	56.32	18.25	−
F	4.86	68.69	26.45	−
G	7.42	42.66	7.56	42.36

compositions is about 20 μm which does not have obvious variety. With the increase of Pr addition, β phase ($Mg_{17}Al_{12}$) morphology changes from the thick bone shape to fine isolated island, and distributes in a non-netlike over grain boundary (Figs.2(a)−(c)). From Fig.2, three secondary phases can be observed in the near-grain boundary. One is lamellar $Mg_{17}Al_{12}$ phase (Figs.2(a)−(c)) near grain boundary which has higher aluminum content. The second is a polygon phase, and EDS analysis shows that it is Mn-rich phase[15] (Fig.2, points *A*, *D*, *G*). The third is needle-like phase and EDS analysis shows that it is Pr-rich phase (Fig.2, points *B*, *C*, *E*, *F*). Considering X-ray and EDS analysis results, it can be concluded that the polygon Mn-rich phase corresponds to Al_6Mn_6Pr, and needle-like Pr-rich phases corresponds to $Al_{11}Pr_3$. With 0.4% Pr addition, fine needle-like $Al_{11}Pr_3$ (Fig.2(a), point *B*) and a small amount of polygon Al_6Mn_6Pr (Fig.2(a), points *A*) phase near the grain boundary can be found in the microstructure. With 0.8% Pr addition, coarse needle-like $Al_{11}Pr_3$ phase (Fig.2(b), point *C*) and coarse polygon Al_6Mn_6Pr phase (Fig.2(b), point *D*) on grain boundary are observed. Further increasing Pr addition to 1.2%, needle-like $Al_{11}Pr_3$ phase (Fig.2(c), point *G*) becomes more coarse, and its size increases obviously. The size of coarse polygon Al_6Mn_6Pr phase (Fig.2(c), point *H*) also increases quickly. $Mg_{17}Al_{12}$ phase morphology changes to be discontinuously net-like.

3.2 Mechanical properties

Table 3 shows mechanical properties of Mg-9Al-*x*Pr alloys. It can be seen that ultimate tensile strength, yield strength, elongation, and hardness are improved while Pr content increases from 0.4% to 0.8%. When the Pr addition increases to 1.2%, the ultimate tensile strength, yield strength, elongation, and hardness have a slight decline.

Fig.3 shows SEM images of tensile fractographs of

Table 3 Mechanical properties of Mg-9Al-*x*Pr alloys

Alloy	σ_b/MPa	σ_s/MPa	η/%	HB
Mg-9Al-0.4Pr	200	105	4.5	64
Mg-9Al-0.8Pr	228	137	6.8	74
Mg-9Al-1.2Pr	222	128	6.2	65

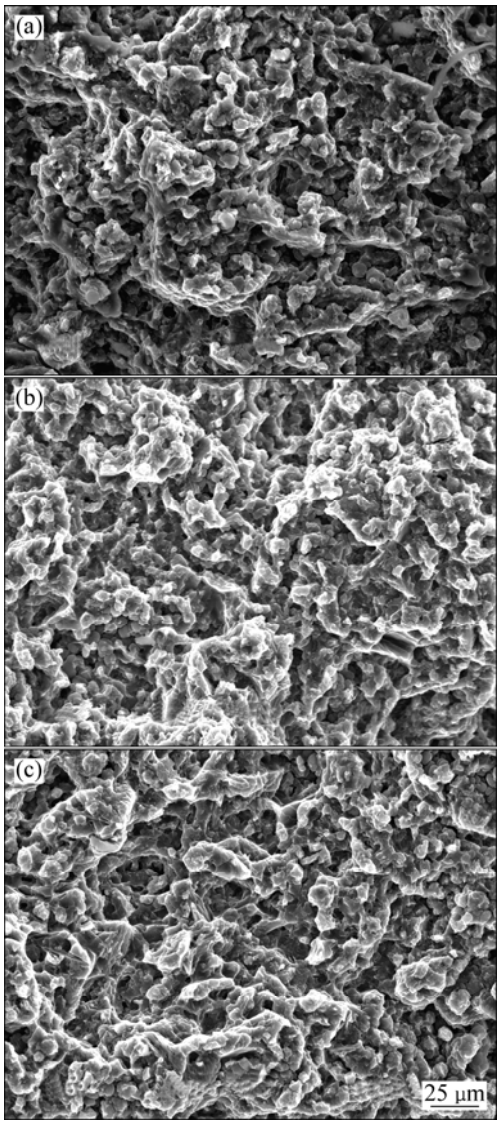

Fig.3 Tensile fractographs of Mg-9Al-*x*Pr alloys at room temperature: (a) Mg-9Al-0.4Pr; (b) Mg-9Al-0.8Pr; (c) Mg-9Al-1.2Pr

Mg-9Al-*x*Pr alloys at room temperature. It can be seen that the tensile fractures of Mg-9Al-*x*Pr alloys are between cleavage fracture and quasi- cleavage fracture, which is as same as the most of Mg-9Al-RE alloys. Both of them have rough surface consisting of many facets and a few second phase particles on facets. By contrasting the fractograph of Mg-9Al-*x*Pr alloys, more small round dimples and tear crackle edges are observed in the fractographs of Mg-9Al-0.8Pr and Mg-9Al-1.2Pr alloy. By comparing the fractographs of Mg-9Al-0.8Pr and Mg-9Al-1.2Pr alloy, it is found that the dimples and tearing edges in fractographs of Mg-9Al-0.8Pr alloy are slightly smaller than those of Mg-9Al-1.2Pr alloy. According to analysis of Mg-9Al-*x*Pr alloy fractographs，the ductility of Mg-9Al-*x*Pr alloys is in accordance with the following order: Mg-9Al-0.8Pr>Mg-9Al-1.2Pr>Mg-9Al-0.4Pr. This result accords with tensile test and

microstructure.

4 Conclusions

The die casting microstructures of Mg-9Al-*x*Pr alloys are mainly composed of α-Mg matrix and $Mg_{17}Al_{12}$. With single Pr addition, $Al_{11}Pr_3$ and Al_6Mn_6Pr phase can be found in the microstructure. With the increase of Pr content, the sizes of Al_6Mn_6Pr and $Al_{11}Pr_3$ phase increase quickly. The increase of Al_6Mn_6Pr and $Al_{11}Pr_3$ phase size can cause a decline in mechanical properties. The mass fraction of 0.8%Pr is considered to be suitable to obtain the optimal mechanical properties.

References

[1] BAKKE P, WESTENGEN H. Die casting for high performance—focus on alloy development [J]. Adv Eng Mater, 2003, 5: 879−885.

[2] LUO A A. Recent magnesium alloy development for elevated temperature applications [J]. Int Mater Rev, 2004, 49: 13−30.

[3] WEI Kun, WEI Liu-ying, WARREN R. Creep behaviour of magnesium die cast alloys AZ91 and AE42 [J]. Material Science Forum, 2007, 546/549: 73−76.

[4] DARGUSCH M S, ZHU S M, NIE J F, DUNLOP G Z. Microstructural analysis of the improved creep resistance of a die-cast magnesium–aluminium–rare earth alloy by strontium additions [J]. Scripta Materialia, 2009, 60: 116−119.

[5] CADEK J , SUSTEK V, KLOC L, EVANGELISTA E. Threshold creep behaviour of an Mg-Zn-Ca-Ce-La alloy processed by rapid solidification [J]. Mater Sci Eng, 1996, A215: 73−83.

[6] WANG Jun, WANG Jian-li, XIAO Wen-long, WU Y M, WANG L M. The microstructure and mechanical properties of Mg-8Zn-8Al-4RE magnesium alloy [J]. Material Science Forum, 2007, 546/549: 187−190.

[7] LIU Wen-juan, CAO Fa-he, CHANG Lin-rong, ZHANG Z, ZHANG J P. Effect ofrare earthe lement Ce and La on corrosion behavior ofAM60 magnesium alloy [J]. Corrosion Science, 2009, 51(6): 1334−1343.

[8] LIU Yao-hui, WANG Qiang, SONG Yu-lai, ZHANG D W, YU S R, ZHU X Y. A study on the corrosion behavior of Ce-modified cast AZ91magnesium alloy in the presence of sulfate-reducing bacteria [J]. Journal of Alloys and Compounds, 2009, 473(1/2): 550−556.

[9] LEE S, LEE S H, KIM D H. Effect of Y, Sr, and Nd additions on the microstructure and microfracture mechanism of squeeze-cast AZ91-X magnesium alloys [J]. Metallurgical and Materials Transactions A, 1998, 29A(4): 1221−1235.

[10] LEE Y C, DAHLE A K, STJOHN D H. The role of solute in grain refinement of magnesium [J]. Metallurgical and Materials Transactions A, 2000, 31A(11): 2895−2906.

[11] BAKKE P, PETTERSEN K, WESTENGEN H. Improving the strength and ductility of magnesium die-casting alloys via rare-earth addition [J]. JOM, 2003, 55(11): 46−51.

[12] WANG Qu-dong, LU Yi-zhen, ZENG Xiao-qin, DING Wen-jiang, ZHU Yan-ping. Study on the fluidity of AZ91+*x*RE magnesium alloy [J]. Materials Science and Engineering A, 1999, 271: 109−115.

[13] FAN J F, YANG G C, CHENG S L, XIE H, HAO W X, WANG M, ZHOU Y H. Surface oxidation behavior of Mg-Y-Ce alloys at high temperature [J]. Metall & Mater Trans A, 2005, 36A(1): 235−239.

[14] RZYCHON T, KIELBUS A. The influence of pouring temperature on the microstructure and fluidity of AE42 alloy [J]. Archives of Materials Science and Engineering, 2007, 28(10): 601−604.

(Edited by CHEN Ai-hua)